Proceedings of the Sixth International Conference on
Railway Technology: Research, Development and Maintenance
Edited by: J. Pombo
Civil-Comp Conferences, Volume 7, Paper 20.4
Civil-Comp Press, Edinburgh, United Kingdom, 2024
ISSN: 2753-3239, doi: 10.4203/ccc.7.20.4

An Adaptable Swivel Button Clamp with Enhanced Fatigue Durability

S. M. Barrans[1], A. Mccarthy[2] and Z. Fazili[1]

[1]Institute of Railway Research, School of Computing and Engineering, University of Huddersfield
Huddersfield, UK
[2]Product Development, Associated Utility Supplies
Huddersfield, UK

Abstract

This paper documents the design analysis and experimental validation undertaken to enable replacement of a galvanized, malleable cast iron swivel clamp button, used within the overhead line system, with a machined from billet, stainless-steel alternative. The German FKM design code is used to assess the durability of both components whilst the experimental work is used to demonstrate the static strength of the stainless-steel button. The analysis demonstrates that the cast iron button may not have the required 6 million cycle durability. Investigation of a failed cast-iron button has indicated that poor casting quality, lack of adherence to design specifications and poor galvanizing may all have contributed to failure. The stainless-steel alternative is predicted to exceed the required life span and provides greater system design flexibility.

Keywords: cast-iron, stainless-steel, FKM method, failure, overhead line, swivel clamp.

1 Introduction

The system of Overhead Line Equipment (OLE) delivers electrical energy continuously to a train as the pantograph on the locomotive is in continual contact with the contact wire. Any loss in contact between the wire and pantograph, will result in degradation of energy transfer to the train [1] and, due to arcing, accelerated wear of the carbon strip on the pantograph (needs ref). To maintain contact the OLE system is held in tension. Additionally, the along track path of the contact wire and messenger

wire are staggered to ensure even wear of the pantograph [2]. Load transfer between the messenger wire and the supporting structure (cantilever, gantry or head-span system) is often via a swivel clamp comprising a clamp attached to a swivel button, as shown in Figure 1. Additional loads on these clamps are also generated within corners in order to force the catenary system to follow a curved path.

Figure 1: Swivel clamp button assembly holding messenger wire.

Within the UK rail network, a large number of swivel clamp buttons currently in use were originally designed in 1966 [3]. These clamp buttons were cast from malleable cast iron and then hot dip galvanized. As detailed below, some swivel clamp buttons have recently failed and need to be replaced. Indeed, some relatively recently installed buttons have failed after only a few years of service. A program of work was therefore undertaken to determine the cause of failure and generate a design which would be more robust whilst still being cost effective.

2 Failure analysis

Figure 2. shows a button clamp which has failed in service, the button head having been lost in the track ballast. The failed surface of the clamp shows a uniform colour and texture, apart from one small region showing a brown discoloration. This indicates the presence of either an inclusion, or a porosity which was not covered by the galvanized coating and hence corroded.

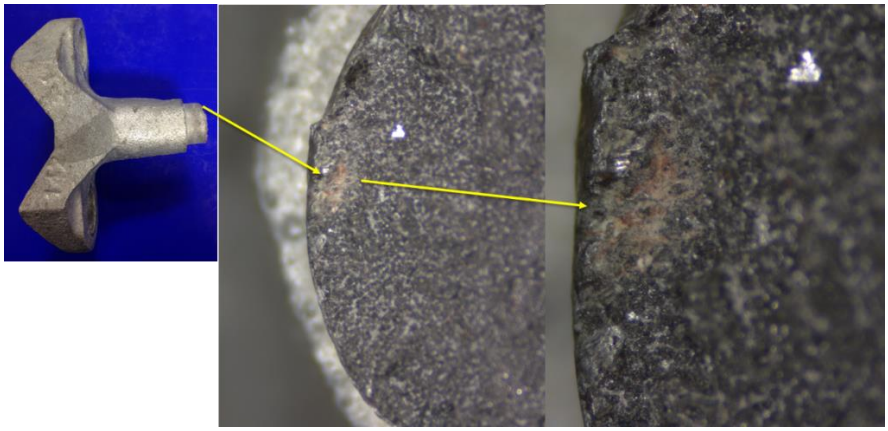

Figure 2: Failed button clamp

Whilst there was no clear indication of a source of cracking, brinelling marks on the surface of the clamp stem, as shown in Figure 3. indicated the area of interaction with the swivel clamp. It was noted that this was coincident with the previously identified inclusion/porosity. These observations suggest that failure was a result of axial loads and horizontal loads being applied to the button simultaneously.

It was also noted that the groove under the button head had not been machined as specified in the drawing but was in the as-cast state.

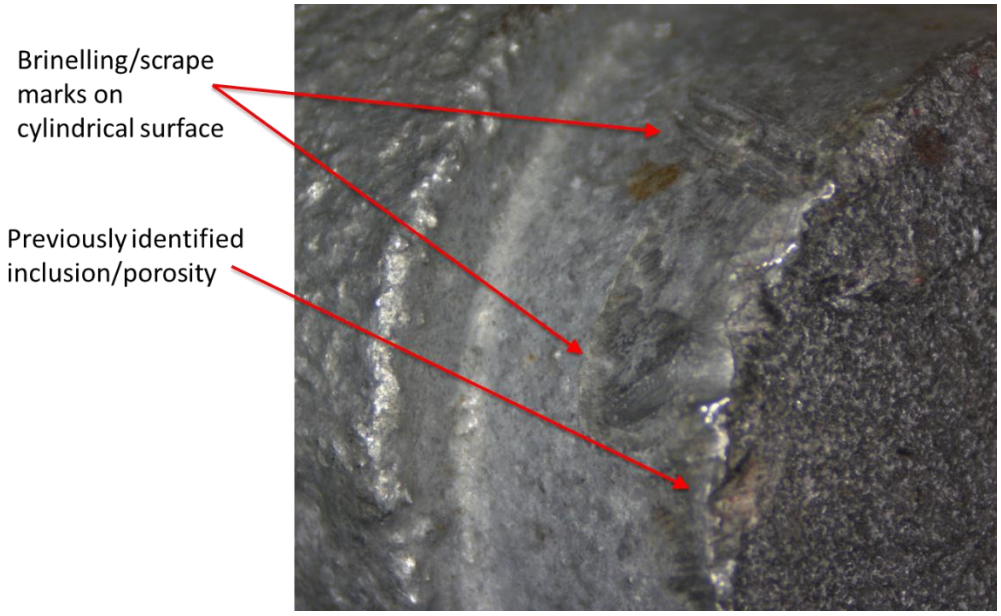

Figure 3: Surface damage on clamp stem

2 Design requirements

Clamp buttons are typically fixed to the tubular structures supporting the overhead line. Within the UK network, these tubes have outer diameters ranging from 42.4 to 60.3 mm. Button head diameters of 25 mm and 38 mm are typically used. In developing the design of a replacement button, flexibility to accommodate the full range of applications was achieved by making button assembly in two parts: the base and the button, as shown in figure 4.

The loads applied to clamp buttons are dependent on the particular application of the button. The applications discussed in this paper are the buttons used to support the contact wire and messenger wire within the UK Master Series. The loads applied to these buttons are derived from a number of factors including wire tension, wire mass, wind loading, ice loading and track corner radius. The derivation of these loads is governed by a number of Network Rail standards [4], [5], [6]. A summary of the parameters from which the loads are derived are given in table 1 for a track speed of 140 mph.

Figure 4: Stainless-steel button and aluminium base assemblies for a range of button and tube sizes.

Parameter	**Value**
Max tension length	750 m
Max span length	65 m
Basic wind velocity	27 m/s
Messenger wire tension	13.0 kN
Messenger wire diameter	10.5 mm
Messenger wire linear weight	5.89 N/m
Ice load – 9.5mm (Nationwide)	5.366 N/m
Contact wire diameter	13.2 mm
Contact wire tension	16.5 kN
Contact wire linear weight	10.5 N/m
Dropper weight	0.458 N/m

Table 1: System parameters

The static working loads revied from these parameters are shown in table 2.

	Messenger wire clip		Contact wire clip
	Vertical (N)	Horizontal (N)	Horizontal (N)
Permanent gravity	1264		
Permanent tension		975	1238
Wind		686.2	690.2
Ice	402.7		
Maintenance	1000		

Table 2: Static loads on catenary system suspension points

For the fatigue loading case, only the permanent loads due to tension and gravity are considered, along with the uplift of the contact wire due to the pantograph which reduces the load on the system. Variable loads due to ice are neglected as firstly, the maximum ice load shown in table 2 is an extreme event and secondly, loading and unloading due to ice is extremely low frequency. Currently, variation in wind load is neglected. Working from [6] the uplift, f, to be considered for fatigue loading is 100

mm. The length, U_l, of contact wire considered to be supported by the pantograph is then determined from equation (1):

$$U_l = \sqrt{\frac{8Tf}{w_{cont}}} \quad (1)$$

Where T is the contact wire tension and w_{cont} is the weight per unit length of the contact wire. The minimum vertical load, V_{min}, on the catenary system is then determined from equation (2):

$$V_{min} = V_{max} - U_l w_{cont} \quad (2)$$

Where V_{max} is the permanent gravity load on the system, taken from table 2. This gives $V_{min} = 807.6$ N. Components forming the catenary system are required to have fatigue lives in excess of 6 million cycles [6].

3 Finite element analysis

Finite element analysis (FEA) was carried out using the simulation facility embedded within SolidWorks. Solid models of the button and base and a mating clamp, demonstrated that there is significant clearance between the parts. This is also observed on the physical parts and is a desirable feature as it allows free rotational movement about the button axis and limited rotational movement about the two perpendicular axes. However, it complicates FEA as, with nominal positioning of the parts, relative rigid body motion is possible. Based on the failure analysis reported in section 1 and knowledge of the loads applied, the SolidModel was manipulated to place the button hard against one side and the bottom of the button socket, as shown in the sectioned view in Figure 5. Contact conditions were then specified to prevent relative rigid body motion.

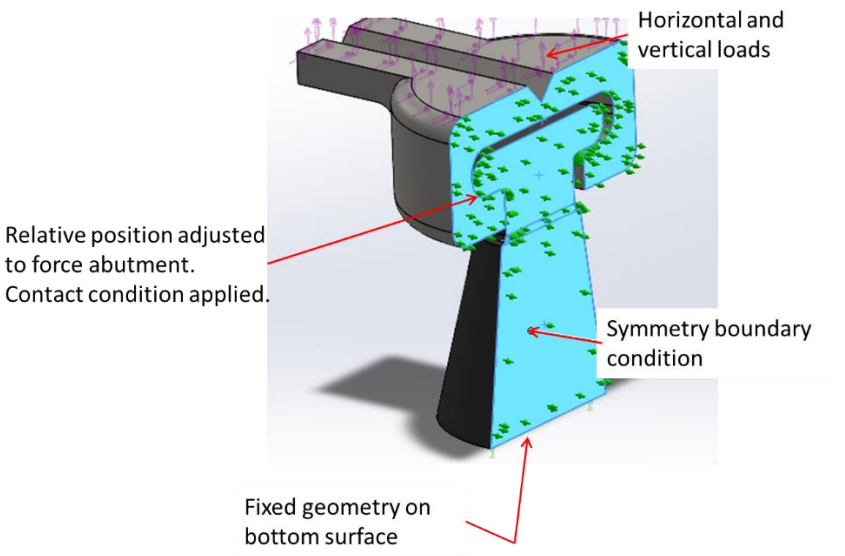

Figure 5: Finite element geometry and boundary conditions

As the focus of the analysis was to design the button to avoid failure, the fact that the clamp is in two halves was ignored. This allowed a symmetry boundary condition to be applied on the sectioned faces of both parts. Also, only the conical section of the button base was included. This allowed the critical stresses under the head of the button to be extracted efficiently. All the initial analyses were carried out using the nominal geometry. Vertical and horizontal loads were applied to the clamp, according to table 2 and the fatigue load specification. These loads were applied as distributed loads to the top surface of the clamp, as shown in figure 5.

Preliminary results from the FEA are shown in figure 6. The high stress where the outer diameter of the button interacts with the socket is to be expected. As the button diameter is smaller than the socket internal diameter, initial contact is at a point. Whilst elastic deformation allows a contact region to be generated, this is still highly localised and hence compressive contact stresses are high. However, as these are compressive stresses, they will not result in fatigue failure.

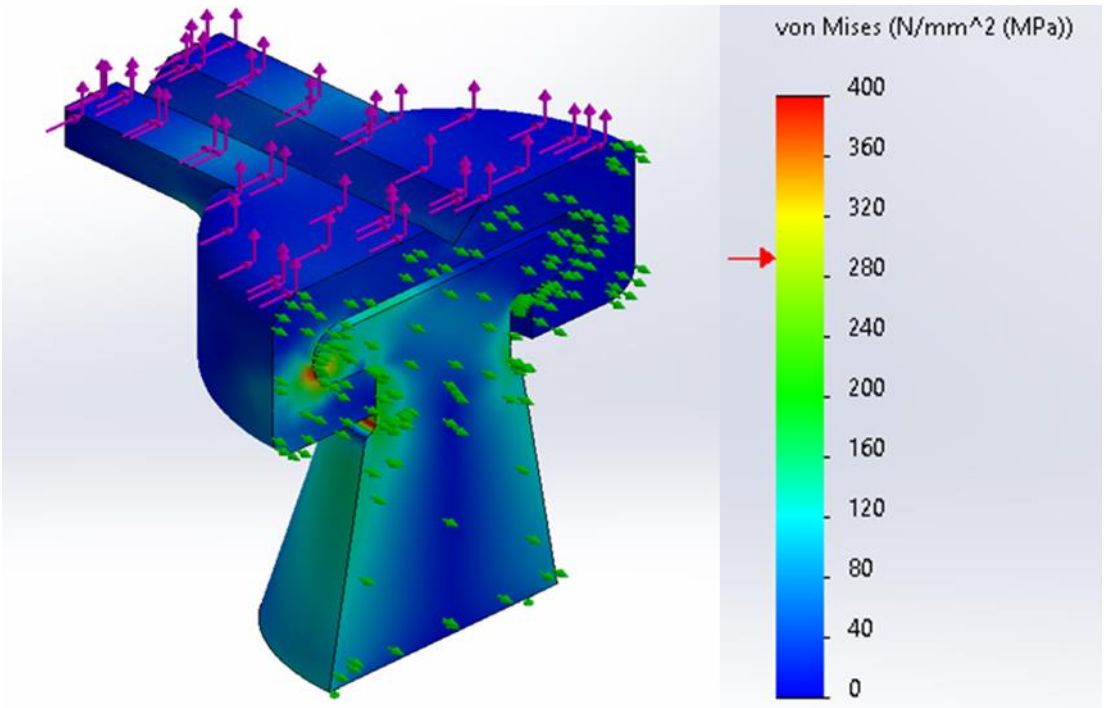

Figure 6. Von Mises stress under maximum vertical load (cast iron button)

An area of high stress is present at the lower fillet radius on the button stem. This is to be expected as the tensile axial stress due to the vertical load will combine with tensile bending stresses due to the horizontal load at this stress concentrating feature. What is notable from this initial analysis is the lack of high stress on the underside of the button where the collected specimen had failed. However, the FEA was based on the nominal geometry with a fillet on both sides of the stem groove whilst the failed specimen did not appear to have the specified fillets.

The stainless-steel button in the new, two-part button assembly screwed into the conical base. A flange with flats was added to facilitate this process, as shown in figure 7. A groove was required under this flange for thread run out. In the initial design, the nominal 0.2 mm radius fillets on this groove gave rise to high stresses.

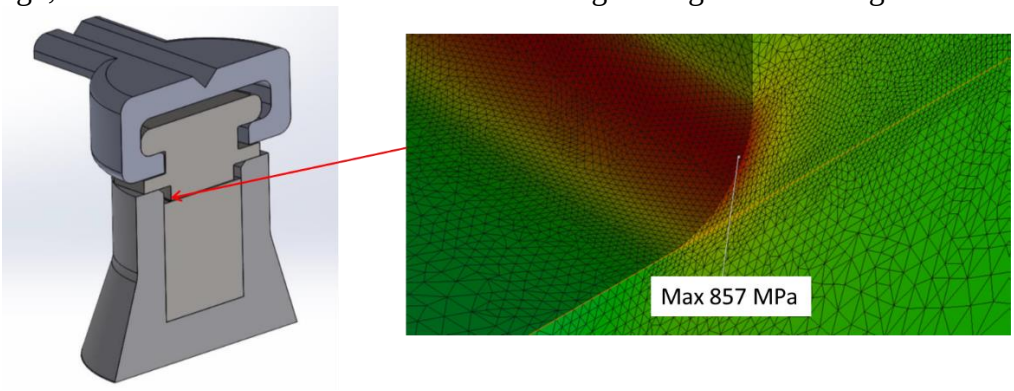

Figure 7: New button assembly, maximum principal stress

Having identified areas of high stress, a mesh convergence study was carried out, based on maximum principal stress. To ensure that the fatigue analysis was robust, this convergence study included stress gradient (see section 4) as well as maximum principal stress.

4 Fatigue analysis

Fatigue analysis of both the cast iron and stainless-steel buttons was carried out using the FKM design code [7], first released in 1994. This method of fatigue analysis takes into account not only the commonly recognised effects of mean stress, stress amplitude, surface roughness, surface treatment and stress concentration, but also accounts for the effect of stress gradient, first recognized by Neuber [8].

From the FEA model, the stress gradient, G_σ is determined by taking the stress amplitude, $\sigma_{1,a,1}$ at the surface node with the maximum first principal stress (node 1) and the stress amplitude, $\sigma_{2,a,1}$ at the next subsurface node (node 2) along a line perpendicular to the surface. The gradient is then determined from:

$$G_\sigma = \left(\frac{1}{\Delta s}\right)\left(1 - \left(\frac{\sigma_{2,a,1}}{\sigma_{1,a,1}}\right)\right) \quad (3)$$

Where Δs is the distance between nodes 1 and 2. From the analyses described in section 3, the values of stress gradient were determined as shown in table 3.

Component	$\sigma_{1,a,1}$ (MPa)	$\sigma_{2,a,1}$ (MPa)	Δs (mm)	G_σ (mm^{-1})
Cast iron button	72.4	69.5	0.0177	2.26
Stainless-steel button	155	137	0.0133	8.85

Table 3: Determination of stress gradient

It should be noted that although the peak stress within the stainless-steel button is high, the stress gradient is also high. The impact of this stress gradient on the

relationship between static stress concentration, K_t, and fatigue stress concentration, K_f, is then accounted for with the factor n_σ, given by equation (4):

$$n_\sigma = 1 + \sqrt[4]{G_\sigma} * 10^{-(a_G + \frac{Rm}{b_G})} \quad (4)$$

Where a_G and b_G are material parameters provided by the FKM code and R_m is the material tensile strength (defined as giving a 97.5% probability of survival).

The static stress concentration can be derived from a substitute structure with a notch of radius, r, and a wall thickness, s. The notch radius can be calculated from the stress gradient according to equation (5). The wall thickness in the cases considered here can be taken as the diameter of the button stem at the point of peak stress.

$$r = \frac{2}{G_\sigma} \quad (5)$$

The static stress concentration is then found from equation (6):

$$K_{t,\sigma} = MAX(10^{0.066 - 0.36 * LOG(r/s)}; 1) \quad (6)$$

This then allows the fatigue stress concentration to be found from equation (7):

$$K_f = K_{t,\sigma} / n_\sigma \quad (7)$$

A surface roughness correction factor is determined from equation (8):

$$K_{R,\sigma} = 1 - a_{R,\sigma} * \log(R_z) * \log\left(2 * \frac{R_m}{R_{m,N,min}}\right) \quad (8)$$

Where R_z is the surface roughness (measured as highest peak to lowest trough), $a_{R,\sigma}$ is the roughness factor material constant and $R_{m,N,min}$ is the minimum tensile strength of the material group. The FKM guide states should $R_{z(DIN)}$ should be used but this is directly analogous to R_{10z} (see [9]) which has been used in this work. The design factor is then determined from equation (9):

$$K_{WK,\sigma} = \frac{1}{n_\sigma}\left(1 + \frac{1}{K_f}\left(\frac{1}{K_{R,\sigma}} - 1\right)\right) \quad (9)$$

Table 4 shows the derivation of the design factor using the data in table 3, the material characteristics and the geometries of the two button designs. The surface roughness for the cast iron button was measured using an Infinite Focus Microscope (IFM) G4 Alicona. The surface roughness of the proposed, machined stainless-steel button was estimated following discussion with the machinist.

Having determined the design factor, the fatigue stress limit for completely reversed stress, σ_{WK}, can be determined from the material fatigue limit for completely reversed stress, $\sigma_{W,zd}$, using equation (10):

$$\sigma_{WK} = \sigma_{W,zd}/K_{WK,\sigma} \quad (10)$$

Design Parameters	**Notation**	**Cast Iron**	**Stainless-Steel**
Kt-Kf Ratio	n_σ	1.960	1.419
Surface Roughness	$R10_z$	76.6 μm	15 μm
Surface Roughness Constant	$a_{R,\sigma}$	0.12	0.22
Minimum Tensile Strength	$R_{m,N,min}$	350 MPa	400 MPa
Surface Roughness Factor	$K_{R,\sigma}$	0.897	0.892
Effective Diameter	d_{eff}	15mm	13mm
Notch Radius	r	0.886	0.226
Wall Thickness	s	7.5	6.5
Static stress concentration factor	K_t	2.511	3.901
Fatigue stress concentration factor	K_f	1.282	2.751
Design Factor	$\boldsymbol{K_{WK,\sigma}}$	**0.556**	**0.736**

Table 4: Calculation of design factor

Where $\sigma_{W,zd}$ can be determined from the tensile strength using a material specific fatigue strength factor, $f_{W,\sigma}$, using equation (11):

$$\sigma_{W,zd} = f_{W,\sigma} R_m \quad (11)$$

As the stress experienced by the buttons does not have a mean of zero, a correction is required, equivalent to the Goodman correction [10]. The mean stress factor, $K_{AK,\sigma}$, is calculated using equation (12):

$$K_{AK,\sigma} = \frac{3+M_\sigma}{3(1+M_\sigma)^2} \quad (12)$$

Where the mean stress sensitivity, M_σ, is found from equation (13):

$$M_\sigma = (a_M 0.001 R_m) + b_m \quad (13)$$

Where a_M and b_M are material constants given in [7].

For cast iron and steel, unwelded components, it is assumed that the endurance limit is 1 million cycles. The variable amplitude fatigue strength, σ_{BK}, is therefore equal to the fatigue amplitude limit σ_{AK}, given by equation (14):

$$\sigma_{BK} = \sigma_{AK} = K_{AK,\sigma}\sigma_{WK} \quad (14)$$

Applying equations (10) to (14) and the appropriate material data leads to the results shown in table 5.

Parameter	**Notation**	**Cast Iron**	**Stainless-Steel**
Tensile strength	R_m	350 [11]	517
Fatigue strength factor	$f_{W,\sigma}$	0.4	0.4
Limiting reversed stress	σ_{WK} (MPa)	252	281
Mean Stress Constants	a_M	0.35	0.35
	b_M	0.13	-0.1
Mean Stress Sensitivity	M_σ	0.253	0.08095
Mean Stress Factor	$K_{AK,\sigma}$	0.691	0.879
Fatigue Amplitude Limit	σ_{AK} (MPa)	174	247
Variable amp fatigue strength	σ_{BK} (MPa)	**174**	**247**

Table 5: Determination of variable amplitude fatigue strength

For cast iron, the FKM code recommends using a safety factor, j_D, of 2.1 and 1.5 for steel where the consequences of failure are severe. Adjusting the variable amplitude fatigue strength using the safety factor and comparing this to the stress amplitude (table 1), allows the degree of utilisation, $a_{BK,\sigma}$, to be determined, according to equation (15), as shown in table 6.

$$a_{BK,\sigma} = \frac{j_D \sigma_{1,a,1}}{\sigma_{BK}} \tag{15}$$

Parameter	**Notation**	**Cast Iron**	**Stainless-Steel**
Safety factor	j_D	2.1	1.5
Stress amplitude	$\sigma_{1,a,1}$ (MPa)	72.4	155
Variable amp fatigue strength	σ_{BK} (MPa)	174	247
Degree of utilisation	$a_{BK,\sigma}$	0.87	0.94

Table 6: Degree of utilisation with nominal design

The degree of utilisation shown in table 6 is less than one in both cases, indicating that both designs should last for more than 1 million cycles. Indeed, since the FKM code assumes an endurance limit for both cast iron and stainless-steel, the analysis is predicting an infinite life for both components.

5 Design investigation

In section 4, it was demonstrated that, according to the FKM standard, both the cast iron and stainless-steel buttons should have an infinite life. It was also shown, in section 3, that the peak stress in the cast iron button was at the lower fillet radius, rather than being close to the observed failure point at the upper fillet radius. However, the FEA reported in section 3 was carried out based on the nominal geometry. Further investigation of the cast iron button was carried out with the upper fillet radius varying

from the nominal 1 mm to 0.05 mm. The results of this investigation are summarised in table 7.

Radius (mm)	$\sigma_{1,a,1}$ (MPa)	G_σ (mm^{-1})	K_f	$K_{WK,\sigma}$	σ_{WK} (MPa)	σ_{AK} (MPa)	Degree of utilisation
0.05	223	26.2	2.19	0.38	368	255	1.819
0.1	171	14.2	1.93	0.42	333	230	1.543
0.2	117	11.0	1.78	0.438	320	221	1.105
0.5	92	4.25	1.49	0.507	276	191	1.005
0.7	82	2.74	1.34	0.541	259	179	0.952
1.0	72	2.26	1.28	0.556	252	174	0.865

Table 7: Cast iron button design investigation

It can be seen in table 7 that the degree of utilisation increases as the fillet radius decreases. For a fillet radius of 0.5 mm, which is the lower tolerance on this dimension, the degree of utilisation is one, indicating that the button has a 97.5% probability of survival. However, for buttons where the fillet radius has not been controlled by machining and may be less than 0.5 mm, there is a significant risk that failure will occur at less than 1 million cycles.

A similar analysis of the impact of fillet radius was conducted for the stainless-steel button. The results of this study are summarised in table 8. It can be seen that once again, decreasing the fillet radius from the nominal 0.2 mm will result in a significant probability of failure within 1 million cycles.

Radius (mm)	$\sigma_{1,a,1}$ (MPa)	G_σ (mm^{-1})	K_f	$K_{WK,\sigma}$	σ_{WK} (MPa)	σ_{AK} (MPa)	Degree of utilisation
0.05	561	33.0	3.96	0.652	317	279	3.02
0.1	213	14.2	3.15	0.706	293	257	1.24
0.2	155	8.92	2.76	0.736	281	247	0.943
0.5	106	3.57	2.11	0.793	261	229	0.693
0.7	94	2.54	1.91	0.814	254	223	0.634
1	82	2.03	1.78	0.828	250	220	0.563

Table 8: Stainless-steel button design investigation

At this point the rationale for the investigated design features should be considered. For both buttons, the fillet radii in the neck region, directly under the button is restricted to a maximum of 1 mm to ensure free movement of the swivel clamp. This places a significant restriction on the design of the cast iron button. However, the stress hotspot region in the stainless-steel button, is the groove machined in the insert to allow for thread run out. The nominal 0.2 mm radius was selected as this matched the cutting tools available at the manufacturer at the time. However, cutting tools with a larger nose radius are readily available and the size of this radius is restricted only by the width of the run-out groove. Allowing a generous radius tolerance of 1 mm to 0.2 mm would ensure a safe design whilst minimising manufacturing cost.

6 Conclusions and Contributions

Failure of cast iron buttons for swivel clamps has been observed on the UK rail network. These clamps were designed in an era when finite element analysis was in the early stage of development and lacked the sophistication required to model the behaviour of interacting parts. Fatigue analysis methodologies have also evolved significantly since this time. A review of the design of this part was therefore required.

This paper has demonstrated how modern FEA packages can be used to determine the stresses arising from the complex interaction between the swivel clamp and the button head. The paper has further illustrated how a modern fatigue analysis methodology can be employed to predict the degree of utilisation the button design. An alternate stainless-steel button design has also been investigated.

The design review has demonstrated that the cast iron button, with the minimum allowable button neck fillet radius, is on the limit of allowable stresses for fatigue. Any further reduction of fillet radius or increase in fatigue loads risks failure of the component within the required 6 million load cycles. Conversely, the critical radius on the stainless-steel button can be easily increased to allow a design with a wide radius tolerance to be produced, all of which would have no significant chance of fatigue failure (i.e. the degree of utilisation would always be well below one).

Acknowledgements

The authors would like thank Innovate UK for supporting this work under KTP project 010705 and University of Huddersfield Capital Venture Fund for supporting the initial investigation.

References

[1] G Keenor, “Overhead line electrification for railways”, 6th ed, United Kingdom, 2021.

[2] A Baxter, “Network Rail A Guide to Overhead Electrification”, 132787-ALB-GUN-EOH-000001, Rev 10, United Kingdom, 2015.

[3] Balfour Beatty Power, “Ball swivel clamp to suit 42.4 and 48.3 tubes”, Drawing No 142/003/A3, United Kingdom, 1991.

[4] “Design of Overhead Line Structures”, NR/L2/CIV/073, Network Rail, United Kingdom, 2015.

[5] “Wind Loading of Overhead Line Equipment and Structures”, NR/L2/CIV/072, Network Rail, United Kingdom, 2019.

[6] “Specification for 25kV A.C. Overhead Contact Line Cantilever Assemblies for Railway Electrification Equipment”, NR/L2/ELP/27428/07, Network Rail, United Kingdom, 2017.

[7] Forschungskuratorium Maschinenbau, “Analytical Strength Assessment of Components in Mechanical Engineering”, 5th ed, VDMA Verlag GmbH, Frankfurt, Germany, 2003.

[8] H Neuber. “Theory of notch stresses”, JW Edwards. Ann Arbor, Michigan. 1946.

[9] L Mummery. “Surface texture analysis the handbook”, Hommelwerke GmbH, Germany, 1990.
[10] RG Budynas, KJ Nisbett, “Shigley’s mechanical engineering design” 11th ed, McGraw-Hill, 2019.
[11] Balfour Beatty Rail Projects, Overhead Electrification Equipment Specification No OEE AKL/156/001, 2009